PAPER

Check for updates

1,4-Azaborine as a controller of triplet energy, exciton distribution, and aromaticity in [6]cycloparaphenylenes†

Jie Wu, [a] Yuhe Kan,*[b] Zhenhua Xue,[a] Jintian Huang,[a] Peng Chen,[a] Xiaofang Yu,[a] Zeyu Guo[a] and Zhongmin Su *[c]

Cycloparaphenylenes (CPPs) have attracted the attention of researchers in various fields because of their unique properties, but studies and applications on host materials in the optoelectronics field are lacking. We undertook preliminary exploration and finally selected 1,4-azaborine and [6]CPP as the basic building blocks to construct a series of BN-[6]CPP hybrids. BN-[6]CPPs with various triplet energies (E_T = 1.66–3.52 eV) could be the potential hosts in full-color phosphorescent organic light-emitting diodes (OLEDs). DFT/TDA-DFT calculations showed that introduction of 1,4-azaborine rings at different positions of the [6]CPP hoop could efficiently control delocalization (localization) of triplet excitons and T_1-state aromaticity (non-aromaticity), and thus varied with the E_T. This work provides not only an efficient strategy for realizing E_T controllability for CPP-based materials by chemical modification of CPP frameworks, but also theoretical guidance for the design and prediction of novel hoop-shaped materials with high E_T in the organic optoelectronics field.

Introduction

In recent years, cycloparaphenylenes (CPPs) have attracted the attention of researchers in various fields because of their unique properties, such as their atomic structure (*i.e.*, geometry, backbone strain, aromaticity, and quinoid character)[1–4] and photophysical properties,[5–11] as well as selective syntheses,[12–14] optical properties in experiments,[15–17] and theoretical modeling.[18–21] Those studies have indicated that most of the properties for CPPs are strongly dependent on the size of the CPP hoop (small, large, odd, or even).[16,22–24]

Small [*n*]CPPs (*n* = 5 and 6) have the obvious quinoid character of the carbon bonds[2] and strong electron delocalization over the whole hoop in the ground (S_0) state, which are

[a] *College of Materials Science and Art Design, Inner Mongolia Agricultural University, Hohhot 010018, Inner Mongolia, People's Republic of China*

[b] *Jiangsu Province Key Laboratory for Chemistry of Low-Dimensional Materials, School of Chemistry and Chemical Engineering, Huaiyin Normal University, Huai'an, 223300, Jiangsu, People's Republic of China. E-mail: yhkan.cn@gmail.com*

[c] *Institute of Functional Materials Chemistry, Faculty of Chemistry, Northeast Normal University, Changchun 130024, Jilin, People's Republic of China. E-mail: zmsu@nenu.edu.cn, zmsu@hotmail.com*

† Electronic supplementary information (ESI) available: The tested T_1 energies at different functionals, molecular orbital correlation diagram, HOMO and LUMO energies, main transition types of the T_1 states, bond length deviations between S_0 and T_1 geometries, NICS(1)$_{ZZ}$ values, and total induced current density plots. See DOI: 10.1039/c7tc02336g

essential for electron transfer and photo-excitation in the CPP hoop, and thereby effective for realizing low-band gap materials. However, small [*n*]CPPs have been confirmed to be unsuitable as luminescent materials, from three main pieces of evidence. First, due to the low band gap, the emission spectrum of small CPPs has been predicted to be in the near-infrared region theoretically but is absent in the visible spectral range in experiments.[18] Second, theoretical calculations have shown the lowest excited singlet (S_1) state to be optically forbidden due to high symmetry, and that the transition density of this state is uniformly smeared around the hoop.[8] Third, the fluorescence quantum yield (Φ) varies significantly with the size of the ring. In particular, the Φ of [6]CPPs is 0.0, indicating that the singlet excited state deactivates by non-radiation transition rather than radiative process.[7,25]

Compared with small CPPs, large [*n*]CPPs (*n* = 9–16) have been shown to be excellent emitters with higher Φ of 0.30–0.90, and the fluorescence maxima become strongly blue-shifted with an increase in molecular size.[5,13,26] This is rationalized by the fact that self-trapping of the lowest excited state due to electron–phonon coupling leads to the formation of spatially localized excitation in large CPPs within 100 fs.[7] This information leads us to ask whether in the T_1 state there is a similar exciton localization on a length scale of several rings in large CPPs and whether the triplet energies increase with increasing CPP hoop size. If so, can large CPPs with high triplet energy (E_T) be used as host materials for phosphorescent organic light-emitting diodes (OLEDs)? Indeed, in larger [*n*]CPPs (*n* = 9–12), the triplet

excitons were confirmed to be localized on several phenyl rings[8] but the E_T shows a slow increase from 1.96 to 2.10 eV, from [9]CPP to [12]CPP.[1,17] The ultra-low E_T cannot meet the most essential requirement of a host material because the E_T of the host must be higher than that of the phosphorescent guest to prevent efficient back-transfer of energy from the guest to the host.[27–29] This is probably the main reason why [n]CPPs and their derivatives have not been studied as host materials. Accordingly, is it possible to construct a host material with high E_T through effective chemical modification of the CPP framework if the size of the CPP is fixed? It has been confirmed that doping of nitrogen into [8]CPP and an increase in nitrogen content has little influence on the distributions and energies of the highest occupied molecular orbitals (HOMOs) and the lowest unoccupied molecular orbitals (LUMOs). Moreover, doping donor–acceptor moieties into the nanohoop can effectively decrease the HOMO–LUMO energy gap.[9,30,31] These results suggest that these doping methods are not conducive to increasing the E_T in the host material.

Based on these findings, we preliminarily conceived that a molecule with a high E_T might have T_1-state localized distribution. Besides, the E_T should be sensitive to the chemical group where the triplet excitons are localized. To meet this requirement, the electron densities first should be asymmetrically distributed at the CPP hoop. How effective is chemical modification of a CPP framework in breaking the symmetry of the CPP hoop and further realizing a wide band gap?

The substitution of one C–C unit of benzene with its isoelectronic BN unit (BN/CC isosterism) gives rise to the three mono-BN substituted benzenes 1,2-azaborine, 1,3-azaborine, and 1,4-azaborine, as shown in Fig. 1. Compared with the parent benzene, azaborines have less aromaticity in varying degrees from 1,2-azaborine to 1,4-azaborine.[32] This feature originates from the fact that the dipolar nature of the B–N unit would significantly alter the electronic properties and intramolecular interactions of the benzene π system due to the different electronegativities and bonding abilities of B and N.[33,34] BN/CC isosterism has emerged as an attractive strategy to expand the chemical space of compounds relevant to biomedical research and optoelectronic materials.[35–41]

This information inspired us to ascertain if the introduction of the B–N unit into the benzene of [n]CPP can break the high delocalization of electrons over the CPP hoop to further help
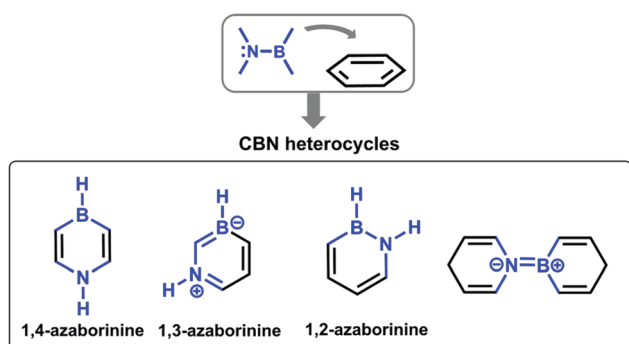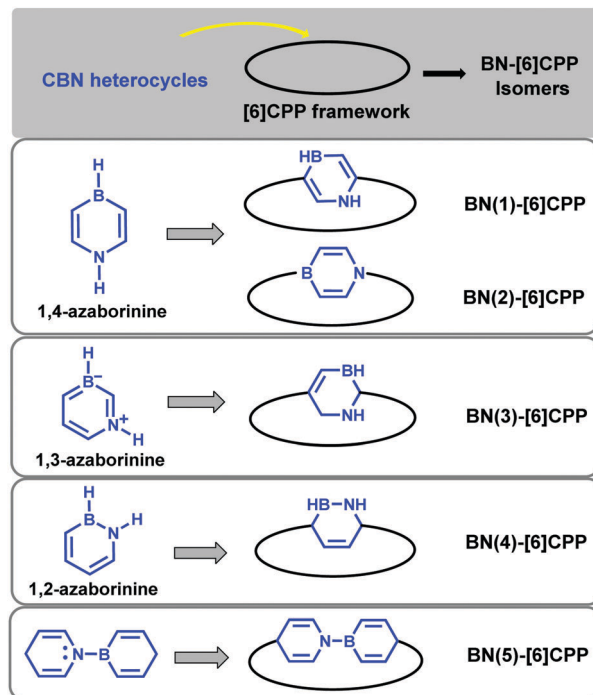
Fig. 2 Five substitution patterns of mono-BN-substituted [6]CPP systems.

localization of T_1 excitons at a side of the CPP hoop. When considering that a large [n]CPP ($n > 8$) or odd-numbered CPP itself may have localization of T_1 excitons, we selected a small and even-numbered CPP (i.e., [6]CPP) as the fixed framework and conceived five possible BN-substitution patterns by introducing a mono B–N unit into a benzene ring (i.e., substitution of a benzene ring with an azaborine unit) or at the bridge between neighbouring benzenes in [6]CPP, as presented in Fig. 2. We investigated the T_1-state properties of the parent [6]CPP, and the results showed that the E_T value was 1.55 eV and the triplet excitons were symmetrically delocalized over the [6]CPP hoop. Then, by judging which pattern can efficiently confine triplet excitons to a side of the [6]CPP hoop and thus improve the E_T compared with that of [6]CPP, we screened out the most optimal BN-substitution pattern as the starting point in our real design of BN-substituted [6]CPPs through quantum-chemical DFT/TD-DFT methods (Scheme 1).

Fig. 1 Four patterns of mono-BN substituted heterocycles.
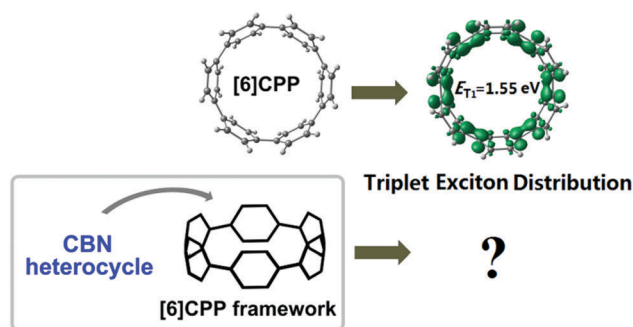
Scheme 1 A design concept for doping mono-BN-substituted heterocycles into the [6]CPP hoop.
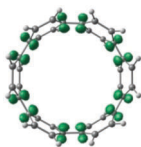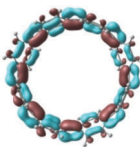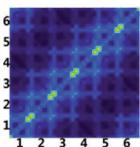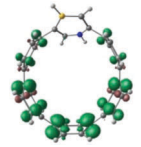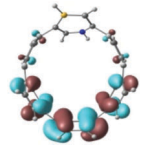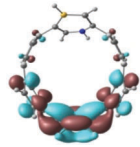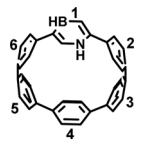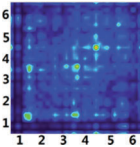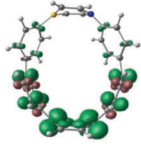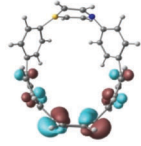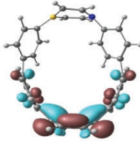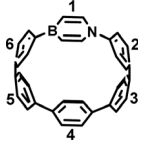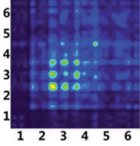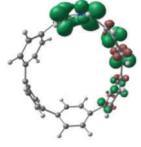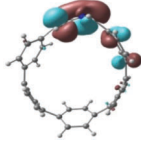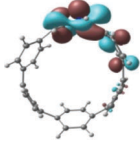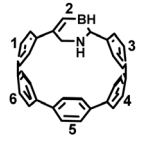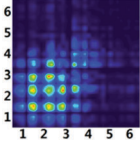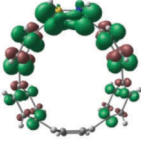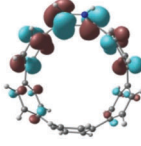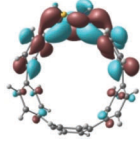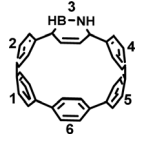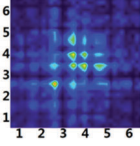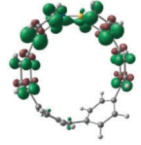
Preliminary exploration: mono-BN-heterocycle-substituted [6]CPPs
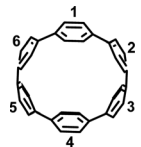
Herein, we started our preliminary exploration. The specific mono-BN-substituted [6]CPP systems and the related data of the electronic properties of the triplet state are given in Table 1. For BN(1)-[6]CPP and BN(2)-[6]CPP (1,4-azaborine-substituted [6]CPPs), the values of E_T (1.66 and 1.67 eV, respectively) were slightly higher than that of [6]CPP. For the other three patterns, (BN(3)-[6]CPP to BN(5)-[6]CPP), the values of E_T (1.47–0.55 eV) decreased in varying degrees compared with that of [6]CPP. Considering the fact that E_T is dominated by distribution of the triplet wavefunction, we carried out a Mulliken population analysis to characterize the spin density distribution of unpaired electrons in the triplet state (*i.e.*, distribution of the triplet exciton). As expected (see Table 1), in all mono-BN-[6]CPP systems, the triplet excitons were asymmetrically distributed at a side of the hoop. The major difference was that the triplet excitons for BN(1)-[6]CPP and BN(2)-[6]CPP (1,4-azaborine-substituted [6]CPP) were mainly localized at the quinquephenyl

moiety, whereas they were at the BN heterocycle and adjacent benzene moieties for the other three patterns (BN(3)-[6]CPP to BN(5)-[6]CPP). These results suggested that the localization of T_1 excitons did not always help the increase in E_T, and t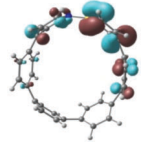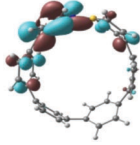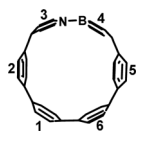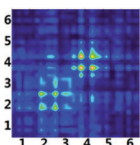hat the E_T largely depends on where the triplet excitons are localized. For example, from the perspective of the distribution of triplet excitons, BN(4)-[6]CPP and BN(5)-[6]CPP are similar to each other, but have a great disparity in the E_T.

Spin density distribution can shed light onto the final distribution of the triplet excitons but cannot provide a detailed description of the excited states. To ascertain the influence of different mono-BN-substitutions at the [6]CPP on the transition nature of the T_1 state, we performed TD-DFT calculations for all mono-BN substituted [6]CPP systems at optimized T_1 geometries. The transition nature and main composition are collected in Table S2 (ESI†). Based on TDA-DFT calculations, the approach of natural transition orbitals (NTOs)[42] was employed to realize the visualization of holes and electrons. Additionally, the transition density matrix (TDM)[43,44] was analyzed to study the spatial span and primary sites of electron transitions. As presented in Table 1,

Table 1 Spin density (SD) distribution, E_T, NTOs, and TDM diagram of mono BN-[6]CPP compounds based on a TDA/LC-ωPBE calculation at the T_1-state geometry. The geometries are marked along the circle in a clockwise direction

Compounds	E_{T1} (eV)	Spin density (isoval = 0.005)	NTO Hole	NTO Electron	Geometry (marked)	TDM
[6]CPP	1.55					
BN(1)-[6]CPP	1.67					
BN(2)-[6]CPP	1.66					
BN(3)-[6]CPP	1.47					
BN(4)-[6]CPP	1.36					
BN(5)-[6]CPP	0.55					

the T_1 excitation for [6]CPP was identified as the local transition (LT) occurring at the carbon atoms between every two neighbouring benzene rings and the coherence was strong. The transitions for BN(1)-[6]CPP and BN(2)-[6]CPP showed the LT to occur within the bent quinquephenyl moiety (ring 2–6), whereas there was little contribution from 1,4-azaborine (ring 1). However, BN(3)-[6]CPP showed an obvious LT between 1,2-azaborine (ring 2) and the neighbouring benzene (ring 3) near B and N atoms. The T_1 transition of BN(4)-[6]CPP showed that the LT mainly occurred between 1,2-azaborine (ring 3) and the two neighbouring benzenes (ring 2 and 4) with a weak coherence between 1,2-azaborine and farther benzenes (ring 1 and 5). In contrast to the findings stated above, for BN(5)-[6]CPP, an obvious charge-transfer (CT) character was visualized in the T_1 transition, which brought about a great decrease in the E_T (0.55 eV) compared with those of all other mono-BN [6]CPP systems. This observation could be attributed to the fact that the large electronegativity difference between B and N atoms of the B–N bond located at the two points of contact between neighbouring benzene rings markedly polarized the [6]CPP hoop into two parts (the donor: B-heterocycle moiety; the acceptor: N-heterocycle moiety). Therefore, the BN-substitution pattern in BN(5)-[6]CPP could not be employed in the molecular design in the next section. The following analyses are only for the azaborine-substituted [6]CPP systems.

To understand why different azaborine substitutions in the fixed [6]CPP framework can bring such different influences on the T_1 transition nature of azaborine-[6]CPPs, we analysed the contribution of molecular orbitals (MOs) to NTOs of holes and electrons. The results indicated that, for four isomeric BN-[6]CPP systems, the contribution to the hole and electron (pairs of NTOs) mainly arose from MO120 and MO121, respectively. Then, we carried out molecular orbital correlation (MOC) for four isomeric [6]CPP systems to ascertain the contributions of each fragment MO to the entire MOs. Four isomeric BN-[6]CPP systems, as depicted in Fig. S2 (ESI†), could be divided into fragment I (azaborine heterocycle) and fragment II (bent quinquephenyl moiety). MOC diagrams show that the contributions to MO120 and MO121 in BN(1)-[6]CPP and BN(2)-[6]CPP basically

arose from the bent quinquephenyl moiety. However, for BN(3)-[6]CPP or BN(4)-[6]CPP, the azaborine and bent quinquephenyl moieties contributed equally to MO120 and MO121. Through the analyses mentioned above, it can be concluded that the introduction of 1,2-azaborine or 1,3-azaborine in [6]CPP caused a strong electronic coupling between the BN-heterocycle and the bent quinquephenyl moiety. This brought about the self-trapping of triplet excitons within the electron-coupling moieties, and consequently the E_T was lower than that of [6]CPP. The strong electronic coupling between the 1,2-, 1,3-azaborine and bent quinquephenyl moiety led to a decrease in the E_T value, so it can be inferred that the E_T value could decrease with an increasing number of 1,2- and 1,3-azaborine rings in the [6]CPP hoop. Therefore, the BN-substitution patterns in BN(3)-[6]CPP and BN(4)-[6]CPP also could not be employed in the molecular design in the next sections. By contrast, introducing 1,4-azaborine into [6]CPP could effectively hinder electron delocalization over the whole hoop, confine the triplet excitons to the bent quinquephenyl moiety, and further improve the E_T value compared with that of [6]CPP. Thereby, the substitution patterns of BN(1)-[6]CPP and BN(2)-[6]CPP could be superior to the other patterns for improving the E_T. Consequently, we selected BN(1)-[6]CPP and BN(2)-[6]CPP as the starting points in our real search for host materials with a high E_T.

Real search

Starting from BN(1)-[6]CPP and BN(2)-[6]CPP, we constructed two sets of BN-[6]CPP derivatives, as displayed in Fig. 3(a) and (b), respectively. In the following sections, all related contents were carried out according to the two parts. Each part was subdivided into two categories according to the different substitution positions of 1,4-azaborine in the [6]CPP hoop. Here, "o" and "p" represent the ortho- and para- positions of substitution in the [6]CPP hoop, respectively. o-nBN-[6]CPP represents the [6]CPP derivative substituted by n 1,4-azaborines at the ortho-positions of the [6]CPP hoop.
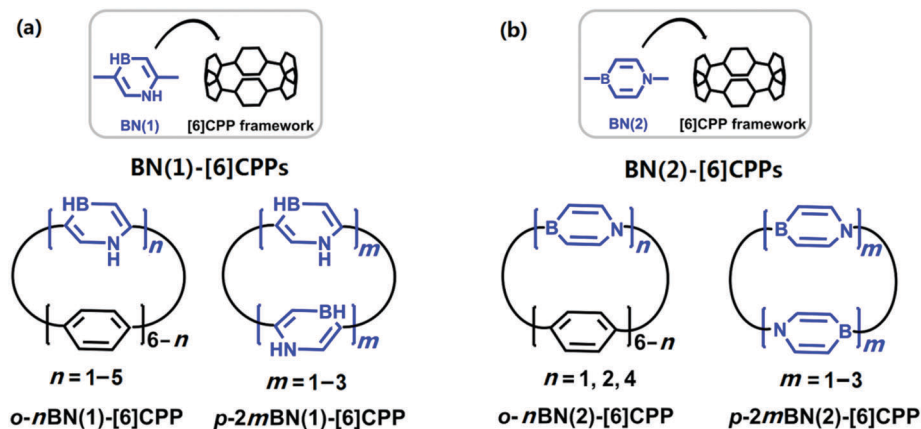

Fig. 3 (a) BN(1)-substituted [6]CPP compounds at the ortho- and para-position of the [6]CPP hoop, respectively. (b) BN(2)-substituted [6]CPP at the ortho- and para-position of the [6]CPP hoop, respectively.

This journal is © The Royal Society of Chemistry 2017

J. Mater. Chem. C, 2017, 5, 9088–9097 | 9091

Taking [6]CPP as a reference, we investigated the variation of the E_T values and the triplet excitons for BN-[6]CPP derivatives with different substitution patterns and the number of 1,4-azaborine rings in [6]CPP, as displayed in Fig. 3. The results for BN(1)-[6]CPPs and BN(2)-[6]CPPs correspond to the right and left parts in Fig. 4, respectively. The right part shows that, from [6]CPP to o-nBN(1)-[6]CPP (n = 1–5), each additional 1,4-azaborine ring could bring a steady increase in the E_T values of approximately 0.07 eV. However, p-2BN(1)-[6]CPP and p-4BN(1)-[6]CPP (1,4-azaborines lay at the para-positions of the [6]CPP hoop) showed a marked increase in the E_T values of 0.43 and 0.77 eV, compared with their isomeric o-2BN(1)-[6]CPP and o-4BN(1)-[6]CPP, respectively. 6BN(1)-[6]CPP had the highest E_T value (3.26 eV) of all BN(1)-[6]CPP derivatives. Similar trends in the evolution of the E_T values were observed for BN(2)-[6]CPP derivatives in the left part of Fig. 4. The main difference was that the increases in the E_T values for BN(2)-[6]CPP derivatives were much more pronounced than those for the corresponding BN(1)-[6]CPP derivatives compared with the parent [6]CPP. Taken together, introducing 1,4-azaborines at the para-positions of the [6]CPP hoop was more efficient than that at the ortho-positions of [6]CPP in improving E_T. Moreover, for p-BN-[6]CPP derivatives (1,4-azaborine substituted [6]CPPs at the para-position of [6]CPP), the E_T values ranged from 2.16 to 3.52 eV.

Visualization of triplet exciton distribution helps explain these trends of the E_T values for all BN-[6]CPP derivatives. From Fig. 4, we find that, in o-nBN-[6]CPPs (including o-nBN(1)-[6]CPPs and o-nBN(2)-[6]CPPs), the triplet excitons were localized at the bent phenylene unit and that the localization area gradually shrank as the number of 1,4-azaborine rings increased. By contrast, the triplet excitons of p-2mBN-[6]CPP (m = 1–3) were delocalized over the entire hoop, with a slight decrease in the spin density around the 1,4-azaborine rings. Especially for p-2mBN(1)-[6]CPP (m = 1–3), the boron atoms made little contribution to the distribution of triplet excitons. Moreover, the triplet excitons of p-2mBN(2)-[6]CPP were dispersed over the entire hoop. In particular, the triplet excitons of 6BN(2)-[6]CPP were evenly delocalized over the entire hoop. Furthermore, bond length deviations (BLDs) between S_0 and T_1 geometries for o-2BN-[6]CPPs (Fig. S4, ESI†) were mainly concentrated on the bent phenylene unit whereas 1,4-azaborine rings were nearly invariable. For p-2BN-[6]CPPs, however, the BLDs appeared in the whole [6]CPP hoop.

A combination of the E_T and distributions of the triplet excitons showed that the delocalization of T_1 excitons over the entire hoop could be superior to the localization of T_1 excitons at the bent phenylene unit for holding a high E_T in two isomeric [6]CPPs (such as p-2BN-[6]CPP and o-2BN-[6]CPP). To provide a rational explanation to this finding, we performed the NTO and TDM analysis based on TDA-DFT calculations.[45]

As presented in Tables 2 and 3, from [6]CPP to o-5BN(1)-[6]CPP (o-4BN(2)-[6]CPP), the T_1 transitions consistently reflected LT within the bent phenylene unit, whereas the coadjacent 1,4-azaborine units formed a collective "defect" and almost did not participate in the T_1 transition.

Therefore, as the number of 1,4-azaborine units increased, the bent phenylene unit gradually shrank and the E_T presented a steady and slow increase. However, for p-2mBN(1)-[6]CPP (p-2mBN(2)-[6]CPP) (m = 1, 2), the T_1 transitions involved the entire hoop and the coherence between pure benzene rings was stronger than that between 1,4-azaborine units and other rings in the [6]CPP hoop. This phenomenon could be because the strong coherence between pure benzene rings in the T_1 state weakened the "hindrance effect" of the 1,4-azaborine unit itself, which brought about participation of 1,4-azaborine units in the T_1 transitions to some extent. Therefore, the E_T values of p-2mBN(1)-[6]CPPs (p-2mBN(2)-[6]CPPs) were noticeably higher than those of o-nBN(1)-[6]CPPs (o-nBN(2)-[6]CPPs) (here, n equals $2m$) due to participation of 1,4-azaborine units with high E_T values
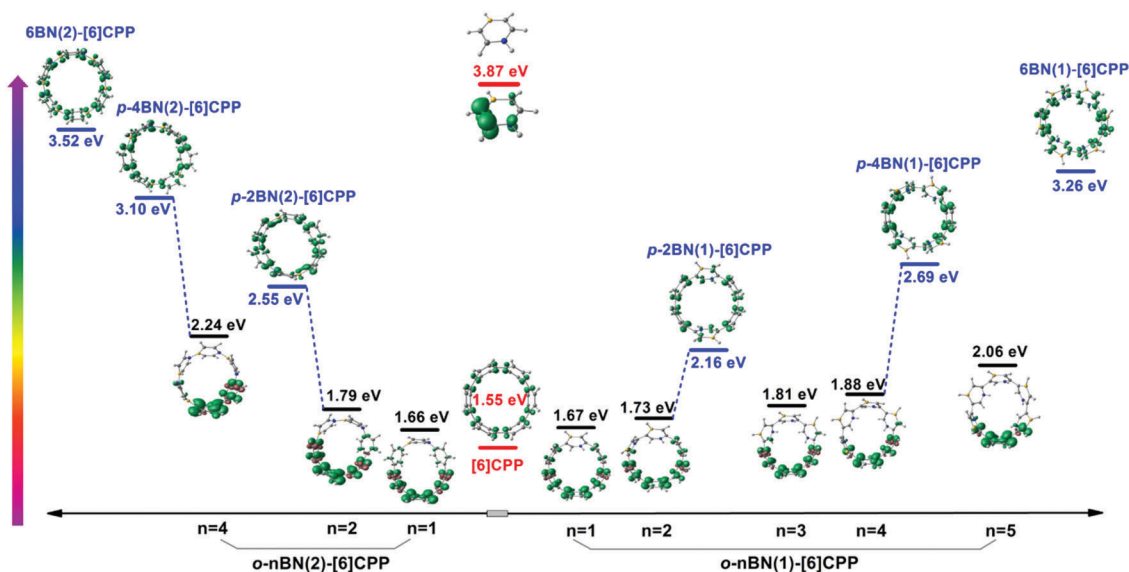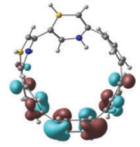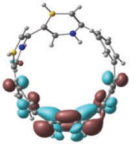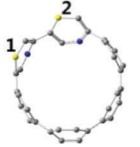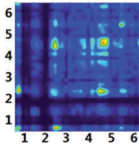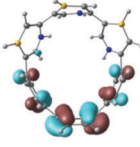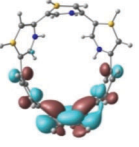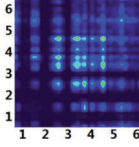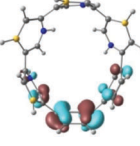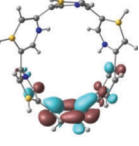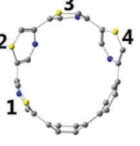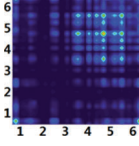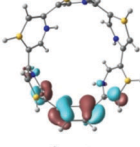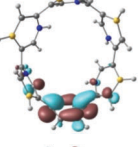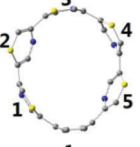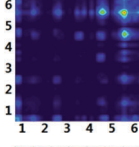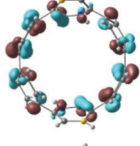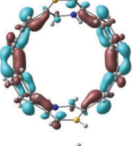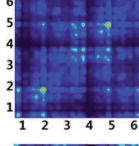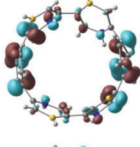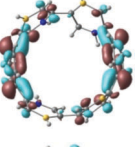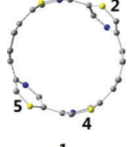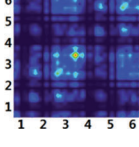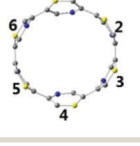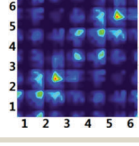

Fig. 4 Triplet energies and spin density distribution for all BN-[6]CPP derivatives.

Table 2 NTOs and TDM diagram of BN(1)-[6]CPP compounds based on TDA/LC–ωPBE calculations at the T_1 state geometry. The geometries are marked along the circle in a clockwise direction
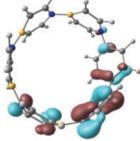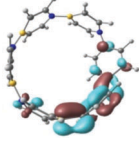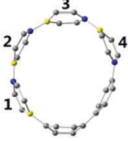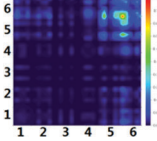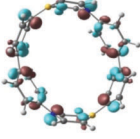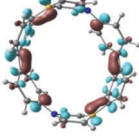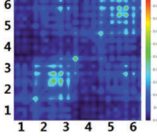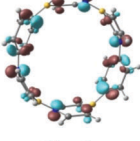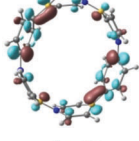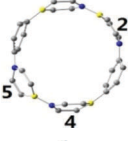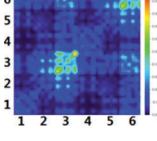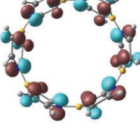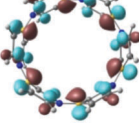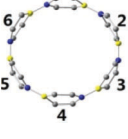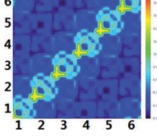
(3.87 eV) in the T_1 state. Moreover, the coherence of the transitions in the whole hoop in p-2mBN(1)-[6]CPP was obviously weaker than that in p-2mBN(2)-[6]CPP. This phenomenon could be because the absence of boron atoms in the transitions weakens the level of electron delocalization at the hoop in p-2mBN(1)-[6]CPP. This hypothesis rationalizes the result that p-2mBN(2)-[6]CPPs have higher triplet energies than the corresponding p-2mBN(1)-[6]CPP. In 6BN-[6]CPP with six 1,4-azaborine rings, the electron-delocalization ability of 1,4-azaborine itself is embodied due to the absence of benzene rings in the hoop. Hence, the TDM diagram for 6BN-[6]CPP showed the strong coherence of the T_1 transitions within the respective 1,4-azaborine rings. Specifically, for 6BN(1)-[6]CPP, there were two parts of the coherences of the T_1 transitions, and each coherence was related to LT between adjacent three rings, and the boron atoms in 1,4-azaborine rings barely participated in

the T_1 transitions. However, for 6BN(2)-[6]CPP, the T_1 transitions not only occurred widely between all 1,4-azaborine rings in the whole hoop (*i.e.*, ICT) but also corresponded to very strong LTs occurring within the respective six 1,4-azaborine rings (*i.e.*, self-trapping of T_1 excitons). Therefore, 6BN(2)-[6]CPP had a higher E_T than 6BN(1)-[6]CPP due to the full participation of 6BN(1)-[6]CPP in T_1 transitions. As concluded above, NTO and TDM analyses fully confirmed the participation of 1,4-azaborine in the T_1 transitions from the viewpoint of types and primary sites of electron transitions, and that the participation of 1,4-azaborine could improve the E_T value because 1,4-azaborine itself has a high E_T.
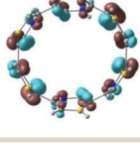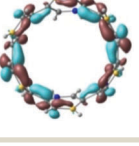
As is well known, sufficient delocalization of electrons at the hoop is necessary for the aromaticity of a molecule. In turn, a molecule with strong aromaticity must surely be a highly delocalized system. Taubert *et al.* reported that [6]CPP with

Table 3 NTOs and TDM diagram of BN(2)-[6]CPP compounds based on TDA/LC-ωPBE calculations at the T_1 state geometry. The geometries are marked along the circle in a clockwise direction
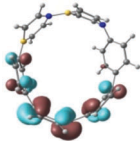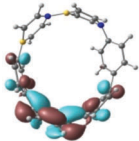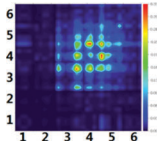
Compounds	NTO		Geometry (marked)	TDM
	Hole	Electron		
o-2BN(2)-[6]CPP				
o-4BN(2)-[6]CPP				
p-2BN(2)-[6]CPP				
p-4BN(2)-[6]CPP				
[6]CPP-6BN(2)				

$4n$ π electrons has a slight antiaromatic character in the S_0 state, with a positive nucleus-independent chemical shift (NICS) value.[46] Baird proposed that the aromaticity in the T_1 excited state should be reversed from that of the S_0 ground state on the basis of the molecular orbital perturbation theory (Baird's rule).[47] This inspired us to investigate whether [6]CPP with $4n$ π electrons has T_1 aromaticity and agrees well with Baird's rule. NICS has been widely used for characterization of the (anti)aromaticity in the S_0 state or excited state.[46,48–52] Herein, we calculated the NICS(1)$_{ZZ}$ values of [6]CPP and BN-substituted [6]CPPs in the T_1 state to investigate the aromaticity of the T_1 state. The NICS(1)$_{ZZ}$ values and total induced current density plots are presented in Table S2 (ESI†). For [6]CPP with $4n$ π-electrons, the NICS(1)$_{ZZ}$ value was positive in S_0 state (10.5 ppm) but negative in the T_1 state (−37.7 ppm), which indicated that [6]CPP had strong aromaticity in the T_1 state but antiaromaticity in the S_0 state, which agrees well with Baird's rule. As new [6]CPP isosteres, BN-[6]CPPs have negative NICS(1)$_{ZZ}$ values to different degrees in the T_1 state. The NICS(1)$_{ZZ}$ values (−25.3 to −10.3 ppm) of p-2mBN-[6]CPPs (m = 1–3) were much more negative than those of o-2BN(1)-[6]CPP and o-2BN(2)-[6]CPP (−1.99 and −4.37 ppm). The more negative the NICS(1)$_{ZZ}$ value, the stronger was the aromaticity. For four isomeric 2BN-[6]CPPs, the strength of aromaticity was estimated to be in the order p-2BN(2)-[6]CPPs > p-2BN(1)-[6]CPPs >> o-2BN(2)-[6]CPP > o-2BN(1)-[6]CPP. We concluded that introducing

1,4-azaborine rings at the *para*-positions of the [6]CPP hoop efficiently preserved the aromaticity of the [6]CPP hoop whereas, at the *ortho*-positions of the [6]CPP hoop, the aromaticity was weakened or vanished. According to the strength of aromaticity, we could judge the relative degree of participation of 1,4-azaborine rings in the electron delocalization and the current pathway in the hoop in the T_1 state, which directly influenced E_T values for different BN-[6]CPPs. Hence, for isomeric BN-[6]CPPs including the same number of 1,4-azaborine units, the stronger the aromaticity, the higher was the E_T value. In addition, as the number of 1,4-azaborine units increased, the E_T value increased and the aromaticity weakened due to the reduction in the number of benzene rings. These trends were well reproduced by a correlation diagram between the aromaticity and E_T value of different BN-[6]CPPs (Fig. 5).

Evaluation of host performance in phosphorescent OLEDs

A higher T_1 energy than that of the phosphorescent guest, as one of the most essential requirements of an ideal host material, can efficiently prevent back-transfer of energy from the guest to the host. For a series of 1,4-azaborine substituted [6]CPPs, the E_T values varied from 1.66 to 3.52 eV with changes in the number of
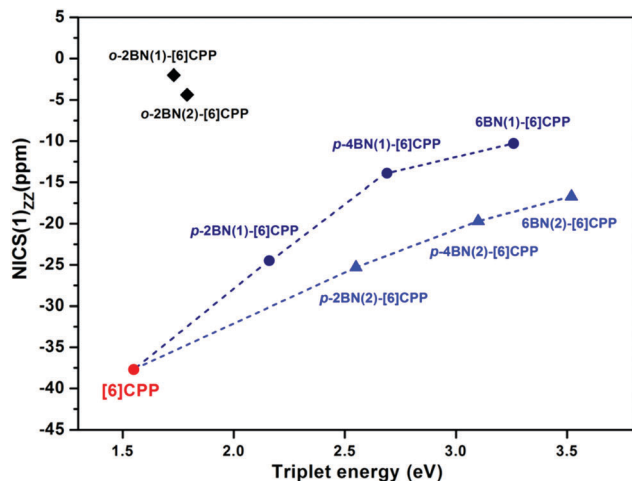
Fig. 5 Correlation diagram between the NICS(1)$_{ZZ}$ and E_T values in [6]CPP and BN-substituted [6]CPPs. The NICS(1)$_{ZZ}$ values are calculated at 1 Å above the hoop center of the [6]CPP hoop using UPBE1PBE/6-31G* at the T_1 geometry.

1,4-azaborine and 1,4-azaborine-substituted positions at the [6]CPP hoop. From the viewpoint of the match of the E_T levels between host and guest, o-nBN-[6]CPPs with E_T values around 2.0 eV as hosts may be more suitable for near-infrared emitting phosphorescent OLEDs. Excitingly, p-2mBN-[6]CPP (m = 1–3) with the E_T values of 2.16–3.52 eV could be the potential hosts in full-color phosphorescent OLEDs.

In addition, a good host material is required to have high HOMO and low LUMO levels for reducing charge injection barriers from neighboring layers and electrodes, thus lowering the driving voltage of the device. As displayed in Fig. S3 (ESI†), the LUMO levels (from −1.11 to −1.79 eV) of p-2mBN-[6]CPPs were lower than that of Alq3 (−1.09 eV) with excellent electron-transporting property. Simultaneously, except for 6BN(1)-[6]CPP, the HOMOs (from −5.33 to −5.67 eV) of the other selected systems were obviously higher than that of mCP (−5.90 eV) with only hole-transporting properties. These features showed that p-2mBN-[6]CPPs (m = 1–3) could be expected to present reduced energy barriers for hole- and electron-injection properties, thus lowering the driving voltage of the device.

Conclusions

This work was carried out progressively according to the principal aim of pursuing high E_T CPP-based materials based on quantum-chemical DFT/TD-DFT calculations. The design process was divided into two stages: preliminary exploration and real search for CPP-based materials with a high E_T. A large amount of preliminary exploration showed that the introduction of only 1,4-azaborine among all mono-BN-heterocycles into a [6]CPP framework could improve the E_T value. In the real search, we designed a series of 1,4-azaborine-substituted [6]CPPs (BN-[6]CPPs). Excitingly, the E_T values varied significantly from 1.66 to 3.52 eV, suggesting that BN-[6]CPPs could be the potential hosts in full-color phosphorescent OLEDs.

We gave an in-depth analysis on the various E_T values for different BN-[6]CPPs, particularly o-BN-[6]CPPs and p-BN-[6]CPPs, from many aspects, such as triplet exciton distribution, triplet transition nature, and T_1 state aromaticity, by employing NTO, TDM, and NICS approaches. Analyses of NTOs and TDM showed that the adjacent 1,4-azaborine rings in o-BN-[6]CPPs presented a collective hindrance effect on electron transitions in the [6]CPP hoop, which led to localization of the triplet excitons at the bent phenylene unit. However, in p-BN-[6]CPPs, the strong coherence between pure benzene rings in the T_1 transitions weakened the hindrance effect of the separated 1,4-azaborine units, which led to the delocalization of triplet excitons over the entire [6]CPP hoop. Distribution of T_1 excitons at 1,4-azaborine units was responsible for the obvious increase in E_T values of p-BN-[6]CPPs compared with parent [6]CPP because 1,4-azaborine itself has a high E_T. Moreover, the NICS values showed [6]CPP and p-BN-[6]CPPs to be isosteres with $4n$ π-electrons having strong aromaticity in the T_1 state but antiaromaticity in the S_0 state, which followed Baird's rule. Moreover, the strength of T_1 aromaticity, which was applied as an indicator of the relative degree of participation of 1,4-azaborine rings in the delocalization of T_1 excitons, rationalized the various E_T values for different BN-[6]CPPs from another perspective.

The present study provides not only an efficient strategy of realizing E_T controllability for CPP-based material by chemical modification of a CPP framework, but also theoretical guidance for the design and prediction of novel hoop-shaped materials with a high E_T in the organic optoelectronics field.

Computational methods

We used density functional theory (DFT) with PBE0 functional[53] and 6-31G* basis sets to optimize ground state (S_0) structures for all molecules that we investigated. The adiabatic E_T values were calculated by means of the ΔSCF method based on the optimized geometries for T_1 and S_0 states. To select a reliable method for calculating the E_T values, in ΔSCF calculations, the stable geometries of S_0 and T_1 states were optimized via DFT and unrestricted DFT methods with a varying fraction of HF exchange, respectively. For comparison, the vertical T_1 energies were calculated based on TDA/LC-ωPBE calculations at the S_0 state geometry (note: TDA/LC-ωPBE is described in detail below). All test results for the seven systems by five methods are presented in Fig. S1a (ESI†). The results indicated that, except for CAM-B3LYP, the other four methods could produce similar evolutional tendencies. The results calculated by the CAM-B3LYP method showed that the E_T for [6]CPP was higher than that of [8]CPP, which was obviously unreasonable. To further verify the reliability of the DFT methods, we estimated the E_T of [n]CPPs (n = 8, 10, 12) by PBE0 and unrestricted PBE0 functional. We concluded from Fig. S1b (ESI†) that, although the PBE0 displayed a slight overestimation of the E_T (about 0.1 eV), the overall trend at PBE0 was similar to that in the experiment. This suggests that the PBE0 method could be used to estimate the relative E_T for CPP-based molecules in our work. Hence,

This journal is © The Royal Society of Chemistry 2017

J. Mater. Chem. C, 2017, **5**, 9088–9097 | **9095**

the spin-unrestricted PBE0 (UPBE0) was adopted to evaluate the stable structures of T_1 states and to calculate the E_T values for all CPP-based systems. A Mulliken population analysis was carried out to characterize the spin density distributions of unpaired electrons in the triplet state to realize visualization of the distribution of the triplet excitons. Based on optimized T_1 geometries, we performed TDA-DFT[45,54,55] calculations using non-empirically tuned range-separated (RS) functionals (LC-ωPBE*) for all systems. For the optimization of the RS parameter ω, all the single-point calculations were carried out for the N and N $\pm$ 1 systems using the default SCF convergence criteria. Therefore, each studied molecule corresponded to a value of ω (see Table S1, ESI†). Based on TDA-DFT calculations, we used the approach of NTOs to realize the visualization of holes and electrons of the T_1 state and plotted the TDM to study the spatial span and primary sites of electron transitions. MOC for representative molecules was analyzed using the Multiwfn program.[56] The NICS(1)$_{ZZ}$ values were calculated at 1 Å above the center of the [6]CPP hoop using the UPBE1PBE/6-31G* at the T_1 geometry. All calculations on the molecules under investigation in this work were performed using the Gaussian 09 program.[57]

Acknowledgements

Notes and references

1 Y. Segawa, H. Omachi and K. Itami, *Org. Lett.*, 2010, **12**, 2262–2265.

2 M. P. Alvarez, P. M. Burrezo, M. Kertesz, T. Iwamoto, S. Yamago, J. Xia, R. Jasti, J. T. L. Navarrete, M. Taravillo, V. G. Baonza and J. Casado, *Angew. Chem., Int. Ed.*, 2014, **53**, 7033–7037.

3 H. Chen, M. R. Golder, F. Wang, R. Jasti and A. K. Swan, *Carbon*, 2014, **67**, 203–213.

4 M. N. Jagadeesh, A. Makur and J. Chandrasekhar, *J. Mol. Model.*, 2000, **6**, 226–233.

5 Y. Segawa, A. Fukazawa, S. Matsuura, H. Omachi, S. Yamaguchi, S. Irle and K. Itami, *Org. Biomol. Chem.*, 2012, **10**, 5979–5984.

6 B. M. Wong, *J. Phys. Chem. C*, 2009, **113**, 21921–21927.

7 L. Adamska, I. Nayyar, H. Chen, A. K. Swan, N. Oldani, S. Fernandez-Alberti, M. R. Golder, R. Jasti, S. K. Doorn and S. Tretiak, *Nano Lett.*, 2014, **14**, 6539–6546.

8 J. Liu, L. Adamska, S. K. Doorn and S. Tretiak, *Phys. Chem. Chem. Phys.*, 2015, **17**, 14613–14622.

9 E. R. Darzi, E. S. Hirst, C. D. Weber, L. N. Zakharov, M. C. Lonergan and R. Jasti, *ACS Cent. Sci.*, 2015, **1**, 335–342.

10 M. Fujitsuka, S. Tojo, T. Iwamoto, E. Kayahara, S. Yamago and T. Majima, *J. Phys. Chem. Lett.*, 2014, **5**, 2302–2305.

11 C. Camacho, T. A. Niehaus, K. Itami and S. Irle, *Chem. Sci.*, 2013, **4**, 187–195.

12 E. R. Darzi, T. J. Sisto and R. Jasti, *J. Org. Chem.*, 2012, **77**, 6624–6628.

13 T. Iwamoto, Y. Watanabe, Y. Sakamoto, T. Suzuki and S. Yamago, *J. Am. Chem. Soc.*, 2011, **133**, 8354–8361.

14 P. Li, B. M. Wong, L. N. Zakharov and R. Jasti, *Org. Lett.*, 2016, **18**, 1574–1577.

15 D. A. Hines, E. R. Darzi, R. Jasti and P. V. Kamat, *J. Phys. Chem. A*, 2014, **118**, 1595–1600.

16 T. Nishihara, Y. Segawa, K. Itami and Y. Kanemitsu, *J. Phys. Chem. Lett.*, 2012, **3**, 3125–3128.

17 M. Fujitsuka, C. Lu, T. Iwamoto, E. Kayahara, S. Yamago and T. Majima, *J. Phys. Chem. A*, 2014, **118**, 4527–4532.

18 V. S. Reddy, C. Camacho, J. Xia, R. Jasti and S. Irle, *J. Chem. Theory Comput.*, 2014, **10**, 4025–4036.

19 J. C. Sancho-García, C. Adamo and A. J. Pérez-Jiménez, *Theor. Chem. Acc.*, 2016, **135**, 25–36.

20 M. R. Talipov, M. V. Ivanov and R. Rathore, *J. Phys. Chem. C*, 2016, **120**, 6402–6408.

21 M. R. Talipov, R. Jasti and R. Rathore, *J. Am. Chem. Soc.*, 2015, **137**, 14999–15006.

22 E. R. Darzi and R. Jasti, *Chem. Soc. Rev.*, 2015, **44**, 6401–6410.

23 K. H. Park, J. W. Cho, T. W. Kim, H. Shimizu, K. Nakao, M. Iyoda and D. Kim, *J. Phys. Chem. Lett.*, 2016, **7**, 1260–1266.

24 Q. Chen, M. T. Trinh, D. W. Paley, M. B. Preefer, H. Zhu, B. S. Fowler, X. Y. Zhu, M. L. Steigerwald and C. Nuckolls, *J. Am. Chem. Soc.*, 2015, **137**, 12282–12288.

25 E. R. Darzi, T. J. Sisto and R. Jasti, *J. Org. Chem.*, 2012, **77**, 6624–6628.

26 M. Fujitsuka, D. W. Cho, T. Iwamoto, S. Yamago and T. Majima, *Phys. Chem. Chem. Phys.*, 2012, **14**, 14585–14588.

27 J. Wu, S.-X. Wu, Y. Wu, Y.-H. Kan, Y. Geng and Z.-M. Su, *Phys. Chem. Chem. Phys.*, 2013, **15**, 2351–2359.

28 J. Wu, Y. Liao, S.-X. Wu, H.-B. Li and Z.-M. Su, *Phys. Chem. Chem. Phys.*, 2012, **14**, 1685–1693.

29 J. Wu, Y.-H. Kan, Y. Wu and Z.-M. Su, *J. Phys. Chem. C*, 2013, **117**, 8420–8428.

30 D. A. Hines, E. R. Darzi, E. S. Hirst, R. Jasti and P. V. Kamat, *J. Phys. Chem. A*, 2015, **119**, 8083–8089.

31 J. M. Van Raden, E. R. Darzi, L. N. Zakharov and R. Jasti, *Org. Biomol. Chem.*, 2016, **14**, 5721–5727.

32 M. Baranac-Stojanović, *Chem. – Eur. J.*, 2014, **20**, 16558–16565.

33 P. G. Campbell, A. J. V. Marwitz and S.-Y. Liu, *Angew. Chem., Int. Ed.*, 2012, **51**, 6074–6092.

34 Z. Liu and T. B. Marder, *Angew. Chem., Int. Ed.*, 2008, **47**, 242–244.

35 X. Y. Wang, J. Y. Wang and J. Pei, *Chem. – Eur. J.*, 2015, **21**, 3528–3539.

36 X. Liu, Y. Zhang, B. Li, L. N. Zakharov, M. Vasiliu, D. A. Dixon and S.-Y. Liu, *Angew. Chem.*, 2016, **128**, 8473–8477.

37 A. Chrostowska, S. Xu, A. Maziere, K. Boknevitz, B. Li, E. R. Abbey, A. Dargelos, A. Graciaa and S. Y. Liu, *J. Am. Chem. Soc.*, 2014, **136**, 11813–11820.

38 T. Zeng, N. Ananth and R. Hoffmann, *J. Am. Chem. Soc.*, 2014, **136**, 12638–12647.

39 S. Xu, T. C. Mikulas, L. N. Zakharov, D. A. Dixon and S. Y. Liu, *Angew. Chem., Int. Ed.*, 2013, **52**, 7527–7531.

9096 | *J. Mater. Chem. C*, 2017, **5**, 9088–9097

This journal is © The Royal Society of Chemistry 2017

40 P. G. Campbell, A. J. Marwitz and S. Y. Liu, *Angew. Chem., Int. Ed.*, 2012, **51**, 6074–6092.

41 Z. Liu, J. S. A. Ishibashi, C. Darrigan, A. Dargelos, A. Chrostowska, B. Li, M. Vasiliu, D. A. Dixon and S.-Y. Liu, *J. Am. Chem. Soc.*, 2017, **139**, 6082–6085.

42 L. M. Richard, *J. Chem. Phys.*, 2003, **118**, 4775–4777.

43 R. McWeeny, *Rev. Mod. Phys.*, 1960, **32**, 335–369.

44 Y. Li and C. A. Ullrich, *Chem. Phys.*, 2011, **391**, 157–163.

45 S. Hirata and M. Head-Gordon, *Chem. Phys. Lett.*, 1999, **314**, 291–299.

46 S. Taubert, D. Sundholm and F. Pichierri, *J. Org. Chem.*, 2010, **75**, 5867–5874.

47 N. C. Baird, *J. Am. Chem. Soc.*, 1972, **94**, 4941–4948.

48 H. Kato, M. Brink, H. Möllerstedt, M. C. Piqueras, R. Crespo and H. Ottosson, *J. Org. Chem.*, 2005, **70**, 9495–9504.

49 V. Gogonea, P. v. R. Schleyer and P. R. Schreiner, *Angew. Chem., Int. Ed.*, 1998, **37**, 1945–1948.

50 J. Oh, Y. M. Sung, W. Kim, S. Mori, A. Osuka and D. Kim, *Angew. Chem., Int. Ed.*, 2016, **55**, 6487–6491.

51 P. B. Karadakov, *J. Phys. Chem. A*, 2008, **112**, 7303–7309.

52 C. J. Kastrup, S. P. Oldfield and H. S. Rzepa, *Chem. Commun.*, 2002, 642–643, DOI: 10.1039/B110626K.

53 J. P. Perdew, K. Burke and M. Ernzerhof, *Phys. Rev. Lett.*, 1997, **78**, 1396.

54 M. J. G. Peach and D. J. Tozer, *J. Phys. Chem. A*, 2012, **116**, 9783–9789.

55 M. J. G. Peach, M. J. Williamson and D. J. Tozer, *J. Chem. Theory Comput.*, 2011, **7**, 3578–3585.

56 T. Lu and F. Chen, *J. Comput. Chem.*, 2012, **33**, 580–592.

57 M. J. Frisch, G. W. Trucks, H. B. Schlegel, G. E. Scuseria, M. A. Robb, J. R. Cheeseman, G. Scalmani, V. Barone, B. Mennucci, G. A. Petersson, H. Nakatsuji, M. Caricato, X. Li, H. P. Hratchian, A. F. Izmaylov, J. Bloino, G. Zheng, J. L. Sonnenberg, M. Hada, M. Ehara, K. Toyota, R. Fukuda, J. Hasegawa, M. Ishida, T. Nakajima, Y. Honda, O. Kitao, H. Nakai, T. Vreven, J. A. J. Montgomery, J. E. Peralta, F. Ogliaro, M. Bearpark, J. J. Heyd, E. Brothers, K. N. Kudin, V. N. Staroverov, T. Keith, R. Kobayashi, J. Normand, K. Raghavachari, A. Rendell, J. C. Burant, S. S. Iyengar, J. Tomasi, M. Cossi, N. Rega, J. M. Millam, M. Klene, J. E. Knox, J. B. Cross, V. Bakken, C. Adamo, J. Jaramillo, R. Gomperts, R. E. Stratmann, O. Yazyev, A. J. Austin, R. Cammi, C. Pomelli, J. W. Ochterski, R. L. Martin, K. Morokuma, V. G. Zakrzewski, G. A. Voth, P. Salvador, J. J. Dannenberg, S. Dapprich, A. D. Daniels, O. Farkas, J. B. Foresman, J. V. Ortiz, J. Cioslowski and G. D. J. Fox, *Gaussian 09, revision D.01*, Gaussian, Wallingford, CT, 2013.

This journal is © The Royal Society of Chemistry 2017

J. Mater. Chem. C, 2017, **5**, 9088–9097 | **9097**